

Application of pseudo-orthogonal codes at the Stimulated-Thermography Non Destructive Testing

by P. Burrascano, L. Senni and M. Ricci*

University of Perugia, Polo Scientifico Didattico di Terni, Strada di Pentima 4, 05100 Terni, Italy,
*corresponding author: marco.ricci@unipg.it

Abstract

Stimulated Thermography is an emerging technique in the field of Non Destructive Testing. In recent years, Pulse Compression based schemes have been proposed to enhance the inspection capability of this technique as well to simplify the experimental set-up allowing the use of low power heating sources that assure higher portability and flexibility. Here a further development of the technique is proposed: by exploiting suitable pseudo-orthogonal codes, a Multi-Input Pulse-Compression Stimulated Thermography scheme is realized. Precisely, multiple heating sources are employed simultaneously and after the application of a proper pulse-compression scheme, the thermal response of the sample under inspection to each source can be retrieved separately. The proposed scheme has been tested on various samples by using both Pseudo-Noise Sequences and Chirp Signals.

1. Introduction: from Pulsed Thermography to Pulse-Compression Thermography

Stimulated or Active Thermography (ST) is an emerging Non Destructive Testing (NDT) technology with application in various fields of research and analysis ranging from diagnostic, material characterization to on-line and in-service inspection [1]. In the last years many techniques have been developed with the aim of gather as much information as possible from the measurement of the thermal response of a system to an external heating stimulus, trying to optimize at the same time the Signal-to-Noise Ratio of the measurement.

In general, any ST procedure can be modeled as the analysis of the Input-Output relation of a system or circuit subjected to a known, controllable, excitation. Moreover the physical Sample-Under-Test (SUT) is usually modeled as a Linear Time Invariant (LTI) system, hypothesis that greatly simplify the analysis by allowing the use of powerful mathematical concepts such as the impulse response and the frequency analysis.

Indeed, for a LTI system/circuit, all the information about the system/circuit itself it is completely embedded in the impulse response $h(t)$: whatever it may be the excitation input signal $x(t)$ used, the output signal $y(t)$ can be predicted by calculating the convolution between $x(t)$ and the system impulse response $h(t)$:

$$y(t) = x(t) * h(t) = \int_0^T x(\tau)h(t - \tau)d\tau$$

where the excitation is defined in the time interval $x(t) \in [0, T]$. The knowledge of the impulse response completely characterized the LTI system and it allows also performing frequency analysis by calculating the transfer function $H(f)$ of the system as the Fourier transform of the impulse response.

Precisely, at each pixel of coordinates (i, j) of a thermal image can be associated a 1-D impulse response $h(t, i, j)$ and from the analysis of these signals inhomogeneities, discontinuities and other geometrical and physical characteristics of the SUT can be inferred.

To measure directly the impulse response of all pixels, the Pulsed ST Thermography was developed so far [2-3]: a single thermal stimulus is applied for a short time (short compared with the typical times of thermal diffusion of the sample) and then, during its cooling, several thermal images are collected. Given a single pixel, the time evolution of its intensity represents its impulse response. As a matter of fact, the main drawback of the method is represented by the maximum amount of thermal energy E_x that one can deliver to the SUT in the excitation time T : if E_x is too small, the noise will overpass the signal during the decay of $h(t)$ erasing the information it carries but, at the same time, E_x cannot be increased arbitrarily. A too high power could damage the SUT as well as induces non-linear phenomena that makes the model no more valid increasing the analysis complexity.

To overcome the problem of a low SNR value the Lock-In-ST was developed [4-6]. In this case the heating stimulus is applied for a long time and its intensity is modulated at a fixed frequency $f_{LOCK-IN}$. By applying the Lock-in analysis on the sequence of thermograms acquired, the response of the system to that frequency is characterized in term of attenuation $A(f_{LOCK-IN})$ and de-phasing $\Delta\varphi(f_{LOCK-IN})$. By this way good values of SNR are achieved even relaxing the heating source requested power for Pulsed-ST that represents a huge obstacle to the practical implementation of the technique. On the other hand, with Lock-In-ST the amount of information about the thermal behaviour of the system is significantly reduced with respect the Pulsed SD since $A(f_{LOCK-IN})$ and de-phasing $\Delta\varphi(f_{LOCK-IN})$ are nothing else that the magnitude and phase of the transfer function at a fixed frequency: $H(f_{LOCK-IN}) = A(f_{LOCK-IN})e^{i\Delta\varphi(f_{LOCK-IN})}$.

Of course, by repeating the Lock-in measurement at various frequencies, an estimation of the whole $H(f)$ can be obtained and then also an estimation of the impulse response $h(t)$. Nevertheless the quality of the estimation depends on

the number of frequencies so that in general this method simply relies on the analysis of the system response to few frequencies properly chosen without considering the time domain analysis. In this perspective, it is worth to ask if it possible to develop a measurement procedure capable of taking the pros of both techniques simultaneously. To accomplish this aim various approaches have been pursued, among which the most effective one is based on the exploitation of coded signals to modulate the thermal excitation and on the use of pulse-compression for the further processing of the acquired thermograms: the Pulse-Compression ST (PuC-ST) [7-11].

Similarly to Lock-In ST, PuC-ST employs a long duration stimulus to deliver enough heat to the SUT but this energy is distributed over a broad frequency range instead of at a single frequency. By applying therefore the pulse compression procedure pixel-by-pixel, the response of the system to a single short heating stimulus, i.e. the set of all $h(t,i,j)$'s, can be retrieved with the optimal SNR values allowed by the measurement conditions. Once estimated the $h(t,i,j)$'s, the relative transfer functions $H(f,i,j)$'s are straightforwardly obtained by applying the Fourier Transform algorithm. For these reasons, PuC-ST is a powerful tool that can be adopted as first step of any active thermal analysis at which make follow a specific processing tailored for the application of interest.

In this paper a further extension of this method is proposed: by exploiting pseudo-orthogonal codes [12-15] as modulating waveforms associated to different heating stimuli, it is possible to simultaneously excite the sample under test with different heating sources and to retrieve, after proper processing on the collected thermograms, the response of the sample to each stimulus separately by introducing a minimum amount of mathematical noise. This opens many new scenarios for PuC-ST since simultaneous excitations can be designed according to several requirements: they can use various physical phenomena (e.g. induction heating and ultrasounds heating in a metallic structure) to study the SUT response with respect to the different type of excitation, they can use excitation frequency range fully or partially overlapping or, as in the present case, they can be provided by absorption of radiation at different wavelengths to reconstruct multi spectral images. Precisely in the experiments reported below, two diode-lasers operating at 830 and 975 nm respectively have been used as heating sources. Moreover both pseudo-orthogonal frequency-modulated and Pseudo-noise codes have been exploited and various samples have been tested.

The paper is organized as follows: the next Section introduces the theory of pseudo-orthogonal codes and their application in Multi-Input Pulse Compression protocols while Section 3 describes in more details the thermography technique developed and the digital processing applied to the data. In Section 4 is illustrated the experimental results and some results are reported, and then in Section 5 some conclusions and considerations about further developments of the technique are drawn.

2. Pseudo-orthogonal codes for Multi-Input Pulse Compression application: Basic principle

Pulse compression is a measurement technique developed for estimating the impulse response $h(t)$ of LTI Systems [16]. Since its development in 60's, due to the benefit it provides, it found a plethora of applications in Radar, Sonar, Optics, Acoustics, Ultrasonics, Eddy Currents up to Thermography [7-11,16-22]. The basic idea at the heart of the technique can be expressed as follows: if exists a pair of signals $\{x[n], z[n]\}$ (henceforth we consider digital signals) such that their convolution is a good approximation of the Dirac delta function, i.e. $x[n] * z[n] = \hat{\delta}[n] \approx C\delta[n]$, the impulse response $h[n]$ of a LTI system can be retrieved by exciting the system with the signal $x[n]$ and then by convolving the system output $y[n]$ with $z[n]$:

$$\begin{aligned} y[n] &= h[n] * x[n] \quad x[n] * z[n] = \hat{\delta}[n] \approx C\delta[n] \Rightarrow \\ y[n] * z[n] &= h[n] * x[n] * z[n] = h[n] * \hat{\delta}[n] \approx C[h[n] * \delta[n]] = Ch[n] \end{aligned} \quad (1)$$

The better the approximation of $\delta[n]$ is, the higher is the quality of the estimation of $h[n]$. Moreover, the theory of matched filter states that, in presence of Additive White Gaussian Noise (AWGN), i.e. when $y[n]=h[n]*x[n]+e[n]$ (where $e[n]$ is the noise term), the choice of $z[n]$ that maximizes the SNR uses the time-reversed replica of the input signal $z[n]=x[-n]$ as the matched filter [23]. With this choice, the approximation $\hat{\delta}[n]$ of $\delta[n]$ coincides with the autocorrelation function $\Phi_x[n]$ of the input signal and, in order to optimize the SNR and to ensure a good measurement resolution, $\Phi_x[n]$ has therefore to be δ -like. This requirement is satisfactorily fulfilled if $x[n]$ is a wideband signal with a bandwidth that spans the entire frequency range of response of the LTI system. Two main families of coded waveforms were developed: (I) frequency-modulated signals and (II) binary Pseudo-noise signals. The linear chirp $x[n] = A \sin(2\pi(f_{start}t + (f_{stop} - f_{start})t^2 / (2T)))$ is the most used waveform of the 1st type, where T is the chirp duration and f_{start} and f_{stop} are the initial and final value of the chirp instantaneous frequency. The 2nd type of excitation contains several different codes but in the present paper the Maximum Length Sequences (MLS) have been used [24]. A more formal description of the pulse compression theory lies beyond the scope of the present paper and the reader is referred to the vast literature on this topic (see for example [17-22]); here we are interested in the possibility of using more simultaneous excitations into a unique pulse-compression procedure with the capability to separate at the end of the procedure the impulse response associated to each input introducing the lowest possible noise. This problem has been studied since 60's by many researchers, especially in the field of radar and of spread spectrum communications, and it was solved by introducing the concept of pseudo-orthogonal codes. Precisely, if exist two or more codes $\{x_1[n], x_2[n], \dots, x_M[n]\}$ all characterized by a δ -like auto-correlation $C\delta[n]$ and having a mutual cross-correlation whose peak value CN is

significantly smaller than C : $CN \ll C$, the set of codes are called pseudo-orthogonal [12-15]. The term pseudo-orthogonal is used because for wideband signals sharing the same bandwidth a perfect orthogonality cannot be reached but their cross-correlation is bounded and so their cross-talk, i.e. noise, is the minimum possible. By exploiting this property it is possible to excite the sample with multiple sources, each modulated by a code of the family. Here, in order to demonstrate the procedure, we limited to two pseudo-orthogonal signals. In this case it can be found that the pseudo orthogonal condition is satisfied for both Chirp and MLS by the pairs of signals consisting of a coded excitation and its time-reversed replica, playing also the role of matched filter [23], that is $x_1[n]=MLS[n]$ or $x_1[n]=Chirp[n]$, $x_2[n]=MLS[-n]$ or $x_2[n]=Chirp[-n]$.

With this choice, the following expressions hold for auto- and cross- correlation of the two waveforms:

	MLS	Chirp
AutoCorrelation	$MLS[n] * MLS[-n] \approx L \times \delta[n]$	$Chirp[n] * Chirp[-n] \approx f_{stop} - f_{start} T \times \delta[n]$
CrossCorrelation	$MLS[n] * MLS[n] \approx \sqrt{L} \times e_{MLS}[n]$	$Chirp[n] * Chirp[n] \approx \sqrt{ f_{stop} - f_{start} T} \times e_{Chirp}[n]$

where L is the length of the MLS code, $|f_{stop} - f_{start}| T$ is the Time-Bandwidth product of the Chirp Signal and $e_{MLS}[n]$ and $e_{Chirp}[n]$ are the mathematical noises with normalized amplitude that take into account the cross-talk between the two sequences.

To have a better insight on how the procedure works, let $h_1[n]$ and $h_2[n]$ be the impulse responses associated to $x_1[n]$ and $x_2[n]$ respectively, the reconstructed impulse responses $\hat{h}_1[n], \hat{h}_2[n]$ after pulse compression will be:

$$y[n] = h_1[n] * x_1[n] + h_2[n] * x_2[n] + e[n] = h_1[n] * x_1[n] + h_2[n] * x_1[-n] + e[n]$$

$$MLS \text{ case : } \begin{cases} \hat{h}_1[n] = y[n] * MLS[-n] \approx Lh_1[n] + \sqrt{L}h_2[n] * e_{MLS}[n] + e[n] * MLS[-n] \\ \hat{h}_2[n] = y[n] * MLS[n] \approx Lh_2[n] + \sqrt{L}h_1[n] * e_{MLS}[n] + e[n] * MLS[n] \end{cases} \quad (2)$$

$$Chirp \text{ case : } \begin{cases} \hat{h}_1[n] = y[n] * Chirp[-n] \approx |f_{stop} - f_{start}| T \times h_1[n] + \sqrt{|f_{stop} - f_{start}| T} \times h_2[n] * e_{Chirp}[n] + e[n] * Chirp[-n] \\ \hat{h}_2[n] = y[n] * Chirp[n] \approx |f_{stop} - f_{start}| T \times h_2[n] + \sqrt{|f_{stop} - f_{start}| T} \times h_1[n] * e_{Chirp}[n] + e[n] * Chirp[n] \end{cases}$$

By using long enough signals the two noise terms, the AWGN and the cross-talk, can be made significantly lower than the true signal, allowing the reconstruction of the two impulse responses with good approximation.

To illustrate the pseudo-orthogonality of MLS and Chirp signals, Figure 1 shows two example of the codes used in the experiments with also the respective auto- and cross- correlation functions.

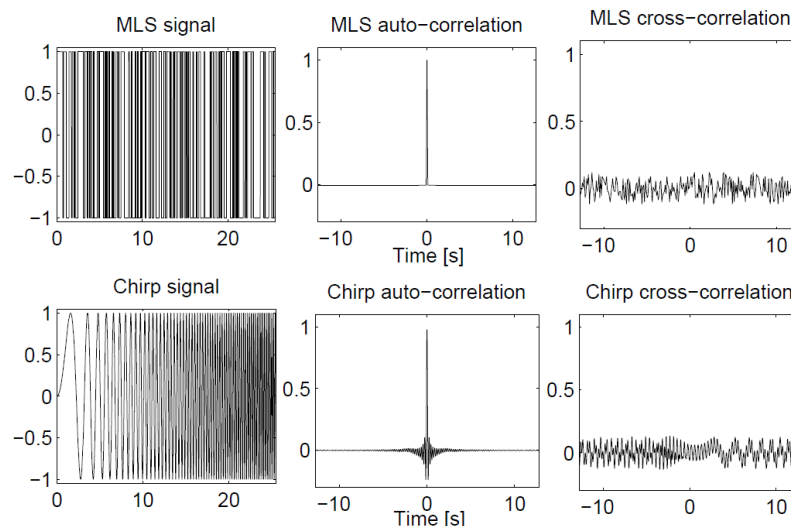


Figure 1. Example of codes used in the experiments. (left) in the 1st row the plot shows an MLS signal of duration $T=25$ s spanning approximately a bandwidth from 0 to 5Hz while in the 2nd row a chirp with the same duration and with $f_{start}=0$ Hz and $f_{stop}=5$ Hz. (center) In the 1st and 2nd row are illustrated the auto-correlation functions of the MLS and Chirp signals respectively. It can be seen that apart a small DC bias, the MLS autocorrelation is almost ideal, while the Chirp autocorrelation presents some sidelobes. These have been reduced in the experiments by introducing an amplitude modulation function on the chirp signal such as the Tukey-Elliptical one []. (right) In the 1st and 2nd row are illustrated the cross-correlation functions of the MLS and Chirp signals respectively. For this choice of the parameters, the noise peak is about 1/10 of the autocorrelation peak but of course can be further reduced by using longer excitations.

3. Pseudo-orthogonal codes for Multi-Input Pulse Compression Simulated Thermography: Measurement Procedure, Set-Up and Signal Processing

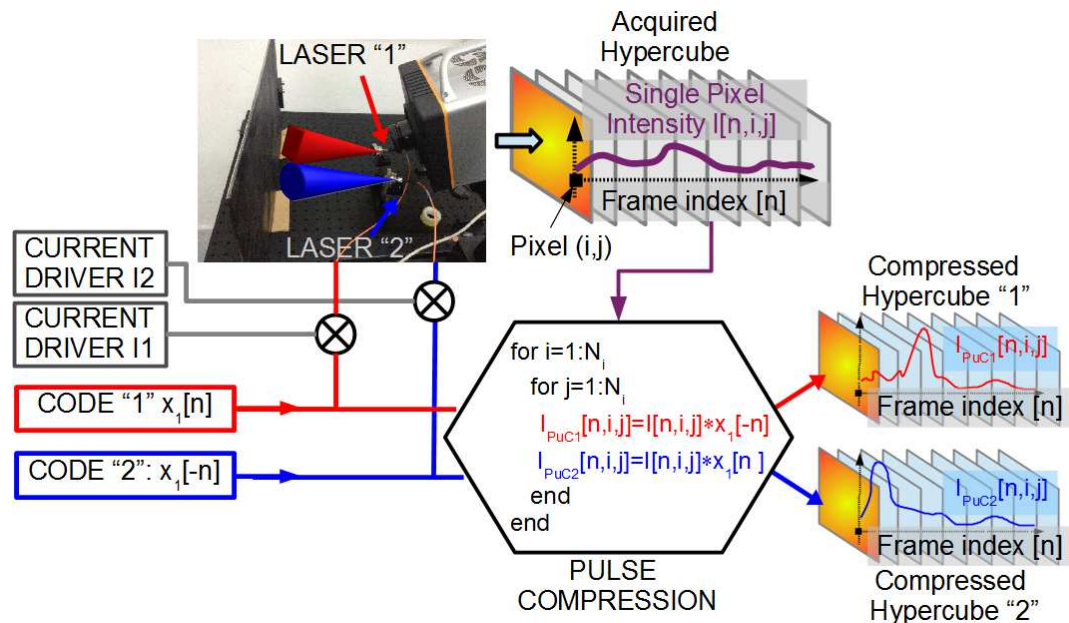


Figure 2. Block diagram of the measurement scheme set-up: two reciprocal MLS sequences modulate the power of two lasers that impinge on a CFRP sample. A single sequence of frames is collected by the camera and then pulse compression is applied for each pixel and for each MLS sequence. At the end two separate sequences are attained

Having introduced the theory of pseudo-orthogonal codes, it is now possible to illustrate in more details how such signals have been used to develop a thermography Multi-Input PuC-ST. A block diagram of the Set-Up is reported in Fig.2: two “pseudo-orthogonal” codes with the same duration simultaneously modulate the power of two diode-lasers operating at 830nm and 975nm respectively from 0 to 1 W. Moreover each laser is equipped with an engineered diffuser coupled with the laser collimator that generate a beam with an almost uniform intensity over a well-defined geometrical area: precisely the 830nm-laser (“LASER 1” in Fig.2) has a square diffuser with a geometrical aperture angle of 20° while the 975nm-laser (“LASER 2” in Fig.2) has a circular diffuser with a geometrical aperture angle of 20°. The two optical beams impinge on the SUT and overlap almost completely. The diffusers have been used to distribute quite uniformly the laser intensity over an area of few centimeters of side and the two different beam geometries have been selected to help the validation of the technique: being each laser associated to a different beam geometry, after the application of the pulse-compression one should be able to reconstruct the impulse response relative to the case in which the laser are switched on one at a time. Moreover the weak peak lasers intensity has been chosen to highlight the benefits that pulse compression provide in term of SNR on the thermal image before and after its application.

The thermograms are acquired by a camera Xenics Onca-MWIR-InSb-320 operating in the wavelength range 3,6-4,9 μm and the frame rate is chosen to be 10-50 higher than the upper frequency of the thermal excitation. For instance, with respect to the signals reported in Figure 1, the frame rate is set in the range 50-250 depending on the wanted time resolution in the reconstructed impulse responses. The collected frames built-up the “Acquired Hypercube” of Fig.2, consisting of the pixel intensity data $I[n,i,j]$ for each pixel (i,j) and frame n . Afterwards, by applying the pulse compression “pixel-by-pixel” as shown in Fig.2, the two “compressed” time sequences of images are obtained, i.e. “Compressed Hypercube 1” and “Compressed Hypercube 2” described by the 3D data $I_{PuC1}[n,i,j]$ and $I_{PuC2}[n,i,j]$ respectively.

It is worth to stress that coded waveforms employed in pulse compression are bipolar signals with almost zero-mean. On the other hand, due to the impossibility of providing with the heating source also a cooling input, the mean heating power delivered to the SUT is not-vanishing and therefore $I[n,i,j]$ is actually the superposition of the response to a step excitation, $I_{DC}[n,i,j]$, with the response to the proper modulated stimulus, $I_{AC}[n,i,j]$, that is $I[n,i,j] = I_{DC}[n,i,j] + I_{AC}[n,i,j]$. The pulse compression should therefore applied correctly to $I_{AC}[n,i,j]$ instead of to $I[n,i,j]$. To accomplish this aim there are two possible strategies: (I) excite the SUT with a periodic stimulus and analyzing the response of a single period once the thermal equilibrium is reached due to the DC component; (II) remove the DC component by using interpolation or high-pass filtering. The former is preferable but in some of the tested cases, due to the low lasers power as well as the low thermal conductivity of the material, the time to reach the equilibrium was too long. In this case it is necessary to use the latter strategy. In the experiments illustrated below, we excited the samples with 3 periods of the coded excitation, and we processed the thermograms relative to the last period. In some cases the thermal equilibrium was reached after 2 periods, in others we removed the DC component. Anyway, since in all the cases the temperature was close to the equilibrium, the fitting of the DC components, and then its removal, was quite easy.

The use of periodic excitation and the consequent analysis of the steady-state response it is also necessary to fully exploit the auto- and cross- correlation properties of MLS for pulse-compression application [25] and it allows the exploitation of the convolution theorem for discrete signals [26]. The cross-correlation of the Acquired Hypercube with the Coded excitations was thus executed in frequency domain as follows:

$$I_{PuC1}[n, i, j] = I[n, i, j] * x_1[-n] = \text{ifft}[\text{fft}(I[n, i, j]) \times \text{fft}(x_1[n])^*] = \text{ifft}[\text{fft}(I[n, i, j]) \times \text{fft}(x_2[n])] = \text{ifft}(A_{PuC1}[k, i, j] e^{\varphi_{PuC1}[k, i, j]})$$

$$I_{PuC2}[n, i, j] = I[n, i, j] * x_2[-n] = \text{ifft}[\text{fft}(I[n, i, j]) \times \text{fft}(x_2[n])^*] = \text{ifft}[\text{fft}(I[n, i, j]) \times \text{fft}(x_1[n])] = \text{ifft}(A_{PuC2}[k, i, j] e^{\varphi_{PuC2}[k, i, j]}) \quad (3)$$

where $\text{fft}(\bullet)$ is the Fast Fourier Transform, $\text{ifft}(\bullet)$ is the Inverse Fast Fourier Transform and $(\bullet)^*$ stands for the complex conjugation.

As intermediate results of the processing reported in Eq.(3), the so-called Amplitude and Phase hypercubes $A_{PuC(a)}[k, i, j]$ and $\varphi_{PuC(a)}[k, i, j]$ are obtained so that also the analysis of the single pixel Transfer Function can be contextually executed. Being $x_1[n]=x_2[-n]$, it is straightforward to see that $A_{PuC1}[k, i, j] = A_{PuC2}[k, i, j]$ so that in the frequency domain the two reconstructed impulse responses differ only for the phase term.

4. Experimental Results

By adopting the measurement procedure previously described, several samples were tested, among which two samples of Carbon Fibre Reinforced Composite (CFRC) with defects consisting in incorrectly displaced fibre and a sample made of polyurethane with air drops inside. The images of the tested samples are reported in Figure 3.

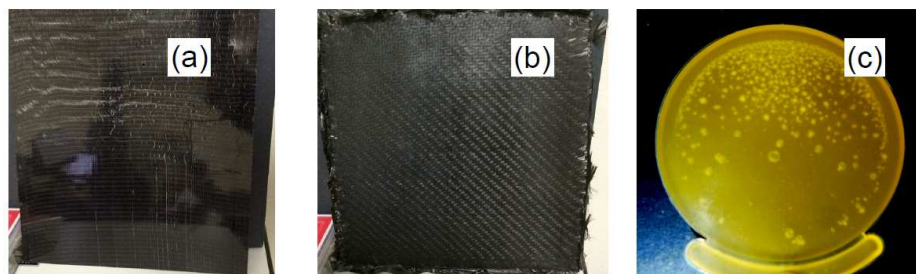


Figure 3 Images of the sample tested: two Carbon Fibre Reinforced Composite (a)-(b), a sample in Polyurethane (c)

First of all, the Pulse-compression procedure was tested for both MLS and chirp excitations to verify the correct working of the set-up. As example, Figures 4 illustrate the results of the Pulse compression by modulating a single laser with MLS and by letting the laser beam, without diffuser, to impinge on the SUT-(a) surface. Without diffuser the beam intensity is high enough to assure that the thermal equilibrium is reached during the first two periods of excitation. Moreover the intensity of a single pixel lighted by the laser shows clearly the heating power modulation waveform. This is also noticed by looking at the thermograms of the acquired hypercube: the intensity of the images pulses with the modulation waveform. On contrary after pulse compression, the entire delivered heat is compressed in a short time and both the single pixel and the hypercube present a very sharp transition corresponding to the onset of the pulse and suddenly a slow decay of the temperature. From the dimensions of the spot after PuC it can be also clearly seen the spatial diffusion of the heat. After this preliminary analysis, the developed procedure and the experimental set-up have been seen to work correctly. Afterwards, by using the diffusers, the sample were inspected by lighting an area with linear dimensions of about 6 cm x 6 cm for the CFRC SUTs and of about 3.5 cm x 3.5 cm for the polyurethane case.

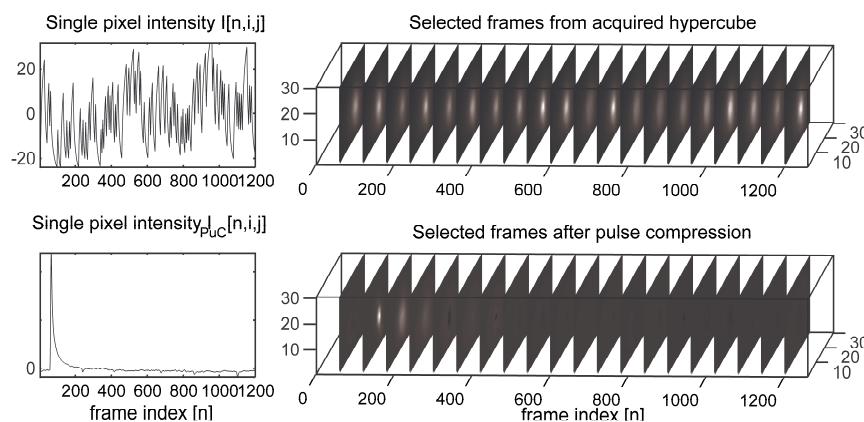


Figure 4 Example of the PuC-ST with a single heating source modulated by MLS codes: (top-left) the time curve of a single pixel intensity during the excitation application; (top-right) some frames from the acquired hypercube; (bottom-left) the time curve of a single pixel intensity after Pulse Compression; (top-right) some frames from the compressed hypercube.

In this case, since the intensity is spread over a large area, the thermal equilibrium is not reached during the excitation so the DC-component of the acquired hypercube was removed before the application of Pulse compression (see Section 3). An example of the procedure applied to a single heating source (“LASER 1”) with the square diffuser and chirp modulation ($f_{\text{start}}=0\text{Hz}$, $f_{\text{stop}}=5\text{Hz}$, Frame Rate= 100Hz , $T=25\text{s}$) is reported in Figure 5.

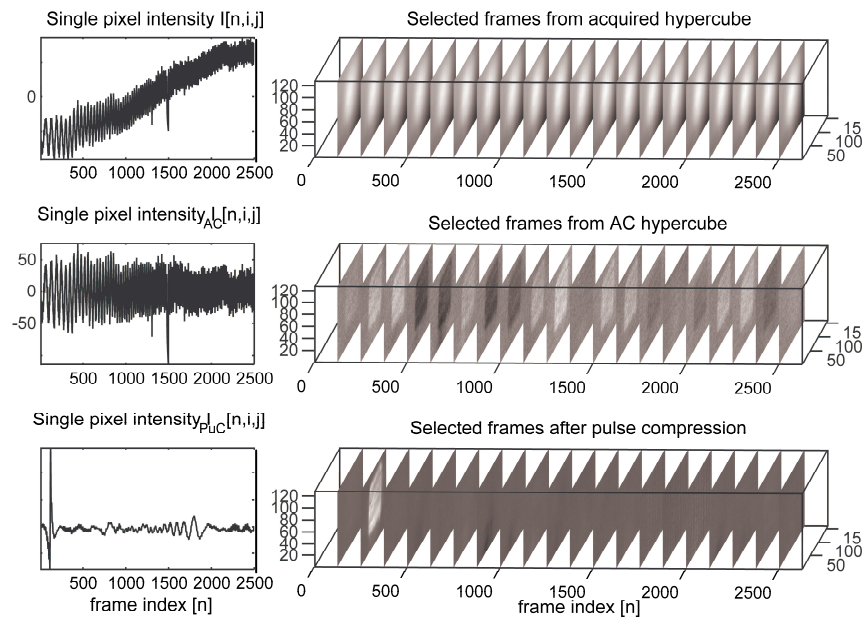


Figure 5 Example of the PuC-ST with a single heating source modulated by Chirp codes with a square diffuser: (top-left) the time curve of a single pixel intensity during the excitation application; (top-right) some frames from the acquired hypercube; (center-left) the time curve of a single pixel intensity after the DC removal; (center-right) some frames from the AC hypercube; (bottom-left) the time curve of a single pixel intensity after Pulse Compression; (top-right) some frames from the compressed hypercube.

Also in this case, even if the single pixel intensity curves are noisy and the images directly acquired exhibit a poor resolution due to the heat diffusion, after pulse compression the images in correspondence of the peak show a high resolution as well as a temporal evolution evidencing the different layers of the composite. This is better seen by focusing on the frames in correspondence of the PuC peak (Figure 6), and by comparing some frames selected from the acquired hypercube with the hottest one after PuC (Figure 7)

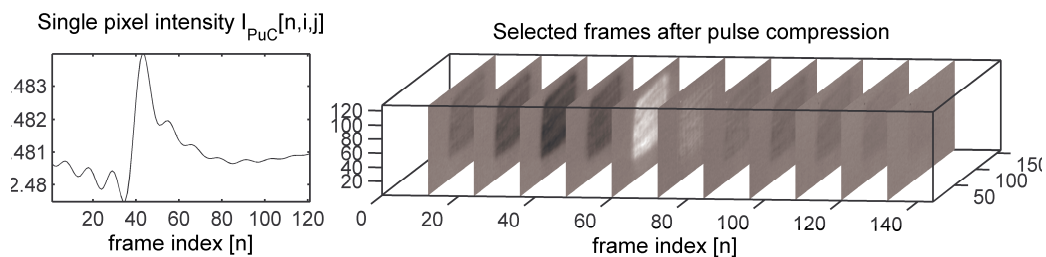


Figure 6 Thermal impulse response of a CFRC reconstructed after Pulse Compression by using “LASER 1” with a square diffuser

As a last step to complete the demonstration of the technique Multi-Input PuC-ST, both lasers were switched on simultaneously and the various SUTs were tested by using both MLS and Chirp signals. As an example, in Figure 8 is shown an overview of the results obtained for SUT-(b) by using two pseudo-orthogonal MLS as modulating function and a square and circular diffuser for “LASER 1” and “LASER 2” respectively. From the plots of the single pixel intensity it can be seen that for both of the compressed hypercubes it is present a sharp peak after pulse-compression at which correspond a thermogram where the expected geometrical shape is retrieved (i.e. square for Compressed hypercube 1 and circular for compressed hypercube 2).

By zooming around the pulse compression peak, a better evaluation of the imaging performances is obtained as illustrated in Figures 9 and 10.

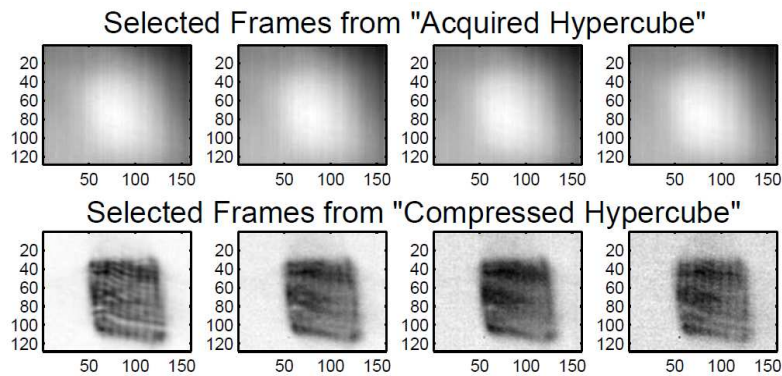


Figure 7 Comparison of some selected thermograms from the Acquired Hypercube and the Compressed Hypercube of SUT-(a) by using "LASER 1" with a square diffuser and Chirp Modulation. While in the former case it is only visible the diffusion of the heat, after pulse compression the illuminated area is clearly visible. Moreover while the 1st frame (the peak of PuC) presents the surface patterns of the sample, in the other frames selected during the decay (see Fig.6) it can be seen the inner structure of the sample.

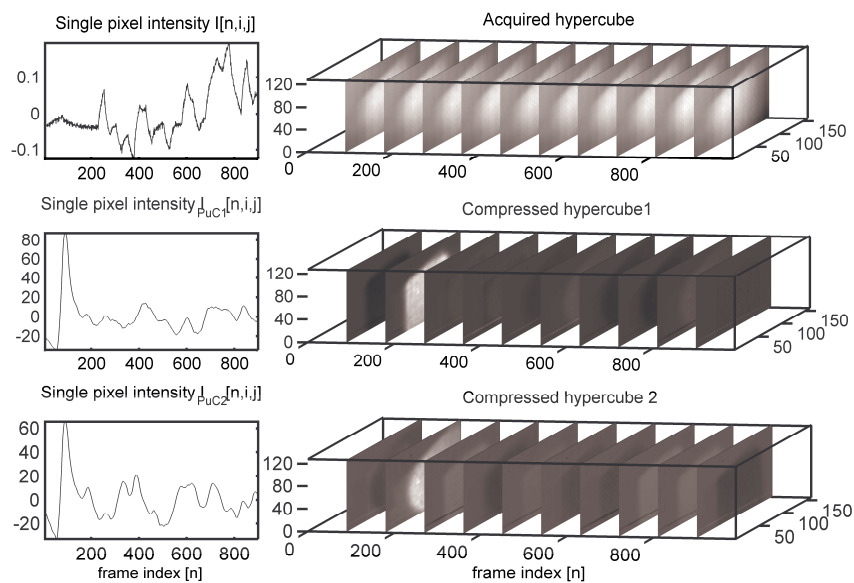


Figure8 Multi-Input PuC-ST with two heating sources modulated by MLS codes with square (LASER 1) and circular diffuser (LASER 2): (top-left) single pixel intensity from acquired hypercube; (top-right) frames from the acquired hypercube; (center-left) single pixel intensity from Compressed hypercube 1; (center-right) frames from Compressed hypercube 1; (bottom-left) the time curve of a single pixel from Compressed hypercube 2; (top-right) some frames from Compressed hypercube 2. ($f_{MAX}=5\text{Hz}$, Frame Rate=50Hz, $T= 50\text{s}$)

Analogously to the case of SUT-(a), the PuC assures images with a high contrast and resolution and the various features of the material (i.e. the wear, the inner layers) are visible. It is worth to stress that the two lasers exhibits different sensitivity: Laser 1 reconstructs better the surface pattern while LASER 2 seems more sensible with respect inner defects as the one circled in red in Figure 11.

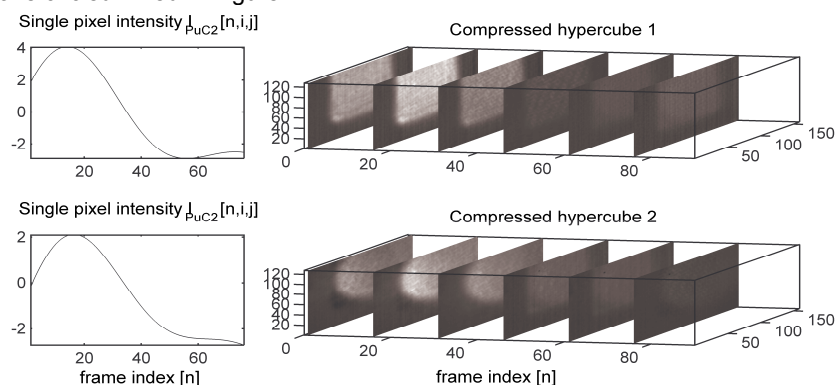


Figure 9 Zoom of Fig.8 around the PuC's peak for Compressed hypercubes 1 and 2

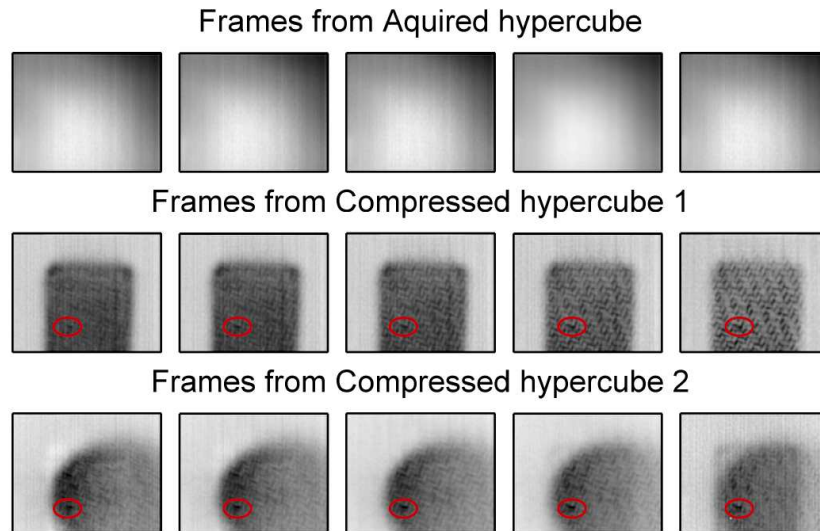


Figure 10 Comparison of selected thermograms from Acquired hypercube and Compressed Hypercubes 1 and 2 for SUT-(b)

This fact highlights the main goal of the Multi-Input PuC-ST procedure: by allowing the simultaneous use of more excitations even based on various physical principles, beside a save of measurement time that can be useful for in-field or in-line applications, different properties of the material can be evidenced and selective heating can be reached. Eventually, the procedure was applied to the SUT-(c) made in polyurethane. The results are reported in Figures 11 and 12. In this case, the SUT adsorbs a very small portion of the radiation and at the same time its thermal conductivity is worst with respect the CFRC samples. The temperature of the sample changed a few during the excitation and it was necessary to heat the sample for a longer time as well as to reduce the bandwidth of the excitation from 5 to 0.5 Hz. Moreover, to identify some defects represented by air-bubbles inside the SUT, the first derivative of the compressed hypercubes was calculated, see Figure 12. It can be seen that also in this case the beam geometries can be retrieved and that also some insight of the inner structure can be gained by the analysis of the thermograms. In particular in correspondence with the area full of air bubbles an anomalous heating is found and also some large bubbles are directly visible in correspondence of the Pulse Compression peak, especially for LASER 1. This once again reinforces the advantage of the technique consisting in a multi excitation allowing a selective heating of the sample.

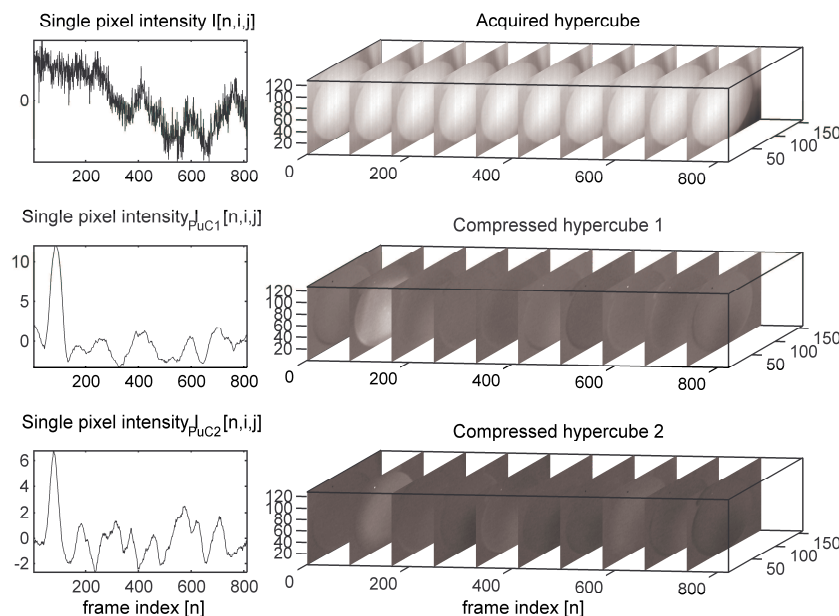


Figure 11 Multi-Input PuC-ST with two heating sources modulated by MLS codes with a square diffuser (LASER 1) and with a circular diffuser (LASER 2) ($f_{MAX}=0.5\text{Hz}$, Frame Rate=25Hz, $T=100\text{s}$)

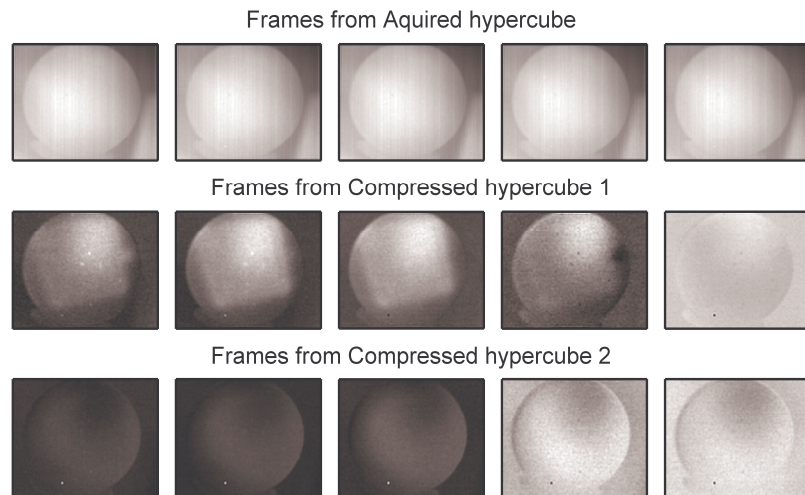


Figure 12 Comparison of selected thermograms from Acquired hypercube and Compressed Hypercubes 1 and 2 for SUT-(c.). The frames are selected once having applied the first derivative to the hypercubes

5. Conclusions

The application of pseudo-orthogonal codes to Pulse-Compression Stimulated Thermography is reported. The technique was successfully tested on various samples and the Pulse Compression procedure was implemented by using both Chirp and MLS signals. The experimental results show that by combining the SNR enhancement provided by Pulse Compression with the possibility of using multiple simultaneous heating sources modulated by pseudo-orthogonal codes, new interesting scenarios are opened: from a multi-spectral thermography where the heating transfer can be made wavelength-selective, to a multi-physics thermography where different heating processes can be exploited to analyze and inspect different parts or different properties of a material. The technique can be further improved by performing contextually frequency analysis and exploiting advanced processing tools such as image fusion and by combining frequency-modulated codes with pseudo-noise codes.

6. Acknowledgements

The authors acknowledge financial support from "Fondazione CARIT".

REFERENCES

- [1] Maldague, Xavier. "Introduction to NDT by active infrared thermography." *Materials Evaluation* 60.9 (2002): 1060-1073.
- [2] Maldague, Xavier, and Sergio Marinetti. "Pulse phase infrared thermography." *Journal of Applied Physics* 79.5 (1996): 2694-2698.
- [3] Maldague, Xavier, François Galmiche, and Adel Ziadi. "Advances in pulsed phase thermography." *Infrared physics & technology* 43.3 (2002): 175-181.
- [4] Busse, G., D. Wu, and W. Karpen. "Thermal wave imaging with phase sensitive modulated thermography." *Journal of Applied Physics* 71.8 (1992): 3962-3965.
- [5] Bai, W., and B. S. Wong. "Evaluation of defects in composite plates under convective environments using lock-in thermography." *Measurement Science and Technology* 12.2 (2001): 142.
- [6] Meola, Carosena, et al. "Non-destructive evaluation of aerospace materials with lock-in thermography." *Engineering Failure Analysis* 13.3 (2006): 380-388.
- [7] Tuli, Suneet, and Ravibabu Mulaveesala. "Defect detection by pulse compression in frequency modulated thermal wave imaging." *Quantitative InfraRed Thermography Journal* 2.1 (2005): 41-54.
- [8] Mulaveesala, Ravibabu, and Suneet Tuli. "Theory of frequency modulated thermal wave imaging for nondestructive subsurface defect detection." *Applied Physics Letters* 89.19 (2006): 191913.
- [9] Mulaveesala, R et al.. "Pulse compression approach to infrared nondestructive characterization." *Review of Scientific Instruments* 79.9 (2008): 094901-094901.
- [10] Mulaveesala, R., and V. S. Ghali. "Cross-correlation-based approach for thermal non-destructive characterisation of carbon fibre reinforced plastics." *Insight* 53.1 (2011): 34-36.
- [11] Tabatabaei, N., and Andreas M. "Thermal coherence tomography using match filter binary phase coded diffusion waves." *Physical Review Letters* 107.16 (2011): 165901.

- [12] Sarwate, D. V., and M. B. Pursley. "Crosscorrelation properties of pseudorandom and related sequences." *Proceedings of the IEEE* 68.5 (1980): 593-619.
- [13] Xiang, Ning, and Manfred R. Schroeder. "Reciprocal maximum-length sequence pairs for acoustical dual source measurements." *The Journal of the Acoustical Society of America* 113 (2003): 2754.
- [14] Golomb, Solomon W., and Herbert Taylor. "Constructions and properties of Costas arrays." *Proceedings of the IEEE* 72.9 (1984): 1143-1163.
- [15] Callegari, Sergio, et al. "From chirps to random-FM excitations in pulse compression ultrasound systems." *Ultrasonics Symposium (IUS), 2012 IEEE International*. IEEE, 2012.
- [16] J. R. Klauder, A. C. Price, S. Darlington and W. J. Albersheim, "The Theory and Design of Chirp Radars," *Bell System Technical Journal* 39, 745 (1960).
- [17] V Schroeder, Manfred R. "Integrated impulse method - measuring sound decay without using impulses." *The Journal of the Acoustical Society of America* 66.2 (1979): 497-500.
- [18] Strickland, D., and Gerard M. "Compression of amplified chirped optical pulses." *Optics Communications* 55.6 (1985): 447-449.
- [19] O'Donnell, Matthew. "Coded excitation system for improving the penetration of real-time phased-array imaging systems." *Ultrasonics, Ferroelectrics and Frequency Control, IEEE Transactions on* 39.3 (1992): 341-351.
- [20] T. H., Hutchins, D. A., Billson, D. R., & Schindel, D. W. (2001). The use of broadband acoustic transducers and pulse-compression techniques for air-coupled ultrasonic imaging. *Ultrasonics*, 39(3), 181-194.
- [21] Choma, Michael, et al. "Sensitivity advantage of swept source and Fourier domain optical coherence tomography." *Optics Express* 11.18 (2003)
- [22] Burrascano, P., Carpentieri, M., Pirani, A., & Ricci, M. "Galois sequences in the non-destructive evaluation of metallic materials". *Measurement Science and Technology*, 17(11), (2006) 2973.
- [23] Turin, G. "An introduction to matched filters." *Information Theory, IRE Transactions on* 6.3 (1960): 311-329.
- [24] Golomb, Solomon Wolf, et al. *Shift register sequences*. Vol. 78. Laguna Hills, CA: Aegean Park Press, 1982.
- [25] Ricci, Marco, Luca Senni, and Pietro Burrascano. "Exploiting Pseudorandom Sequences to Enhance Noise Immunity for Air-Coupled Ultrasonic Nondestructive Testing." *Instrumentation and Measurement, IEEE Transactions on* 61.11 (2012): 2905-2915.
- [26] Hunt, B. "A matrix theory proof of the discrete convolution theorem." *Audio and Electroacoustics, IEEE Transactions on* 19.4 (1971): 285-288.